catena-Poly[[bis(acetonitrile-κN)-manganese(II)]-bis(μ-trifluoromethanesulfonato-κ²O:O′)]

Martin Lutz,[a]* Antoine M. M. Schreurs,[a] Anthony L. Spek,[a] Marcel A. H. Moelands[b] and Robertus J. M. Klein Gebbink[b]

[a]Bijvoet Center for Biomolecular Research, Crystal and Structural Chemistry, Faculty of Science, Utrecht University, Padualaan 8, 3584 CH Utrecht, The Netherlands, and [b]Debye Institute for Nanomaterials Science, Chemical Biology and Organic Chemistry, Faculty of Science, Utrecht University, Padualaan 8, 3584 CH Utrecht, The Netherlands

Correspondence e-mail: m.lutz@uu.nl

The title compound, $[Mn(CF_3SO_3)_2(CH_3CN)_2]_n$, has an Mn[II] cation on an inversion centre in an octahedral environment. The trifluoromethanesulfonate anions act as bridging ligands and form a one-dimensional coordination polymer in the direction of the a axis. The F atoms of the trifluoromethanesulfonate anions form layers parallel to the ab plane, but despite short intermolecular distances, no stabilizing F···F interactions are detected. The Mn—N and C—C bonds of the acetonitrile ligand are analyzed according to the Hirshfeld rigid-bond test. Renninger effects in the reflection data are considered, explored and discussed.

Comment

The title compound, (I), was prepared as a starting material for complexation reactions with biomimetic ligands. In the literature, the stoichiometry of the compound is given as $Mn(SO_3CF_3)_2 \cdot CH_3CN$ (Bryan & Dabrowiak, 1975), but also contains indications of a variable composition. The present crystal structure determination proves the presence of two coordinated acetonitrile molecules and thus the composition $[Mn(SO_3CF_3)_2 \cdot 2CH_3CN]_n$, with the manganese in a 2+ oxidation state (Fig. 1).

The Mn[II] ion in (I) is located on an inversion centre and surrounded by six donor atoms in a slightly distorted octahedral geometry. The equatorial plane is formed by four O atoms of the trifluoromethanesulfonate anions, with Mn—O distances in the expected range for Mn[II]. The axial positions are occupied by acetonitrile ligands, with similar Mn—N distances to those observed in the $[Mn(CH_3CN)_6]^{2+}$ cation (Weller *et al.*, 1996). Due to the inversion symmetry, the equatorial plane is exactly planar and the axial donor atoms

are exactly *trans*. Consequently, the angular variance (Robinson *et al.*, 1971) is very small $(0.75^{\circ 2})$. The slight octahedral distortion can be seen in the small difference between Mn—O and Mn—N distances.

(I)
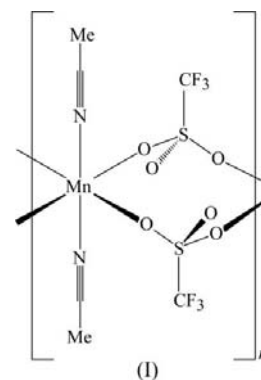
The trifluoromethanesulfonate anions, which are located on general positions, act as bridging ligands between the Mn[II] cations. Bridging trifluoromethanesulfonate anions occur mainly in copper and silver complexes. In fact, there is only one previously known Mn complex with a bridging trifluoromethanesulfonate anion (Berben & Peters, 2008), but there the bridging is supported by an additional bridging isopropoxide linker, resulting in a discrete binuclear complex. In (I), the Mn[II] cations are connected only by trifluoromethanesulfonate anions. In this way, a one-dimensional chain is formed in the direction of the crystallographic a axis. The distance between the Mn[II] ions in the chain therefore corresponds to the length of the a axis [5.13763 (8) Å]. The S—O distances of the coordinated O atoms are about 0.03 Å longer than that of the noncoordinated O atom. The CF_3 group
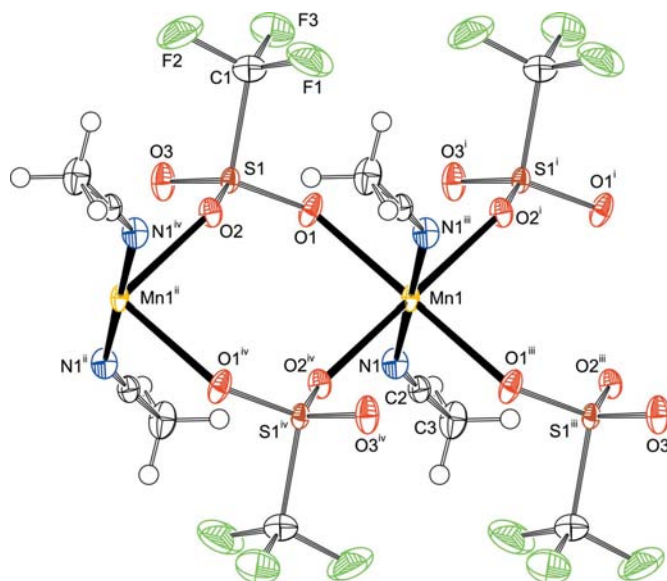
Figure 1
The coordination environment of Mn1 in (I), showing the atom-numbering scheme. Displacement ellipsoids are drawn at the 50% probability level and H atoms are shown as small spheres of arbitrary radii. [Symmetry codes: (i) $x - 1, y, z$; (ii) $x + 1, y, z$; (iii) $1 - x, 1 - y, 1 - z$; (iv) $2 - x, 1 - y, 1 - z$.]
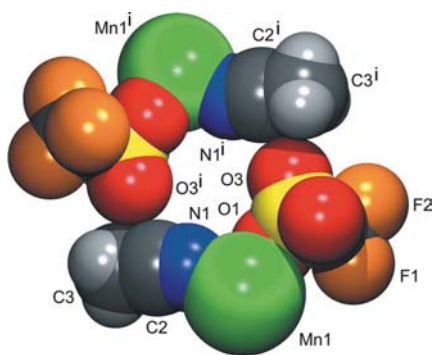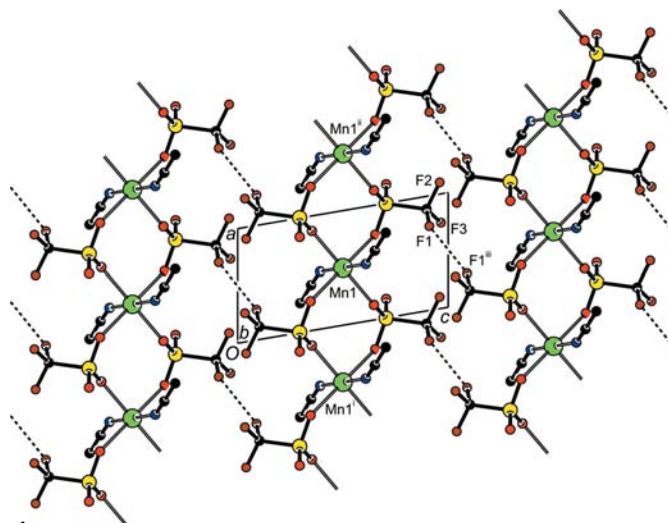
Figure 2
Space-filling plot of (I), showing the close intermolecular contacts between atoms O3 and C2^i, which prevent a linear coordination of the acetonitrile ligands. [Symmetry code: (i) $2 - x, -y, 1 - z$.]

Figure 3
The packing of (I) in the crystal structure, viewed along the b axis, showing the one-dimensional coordination chains in the a direction and the fluorine layers in the ab plane. Short F$\cdots$F interactions are shown as dashed lines. [Symmetry codes: (i) $x - 1, y, z$; (ii) $x + 1, y, z$; (iii) $1 - x, 1 - y, 2 - z$.]

adopts a staggered conformation with respect to the SO$_3$ group.

While in most transition metal complexes of acetonitrile the coordination is approximately linear, (I) deviates significantly from linearity by 26.73 (9)° at the N atom. Previous cases of such a bent coordination mode have been ascribed to crystal packing effects or steric hindrance with neighbouring groups (Murthy *et al.*, 2001). Indeed, the crystal structure of (I) has a packing index of 69.0% (Kitajgorodskij, 1973), indicating an efficient arrangement of the molecules (Dunitz, 1995). The C2$\cdots$O3$(2 - x, -y, 1 - z)$ distance is 3.1612 (15) Å, which is approximately the sum of the van der Waals radii (3.22 Å; Bondi, 1964), and this prevents linearization of the acetonitrile coordination (Fig. 2). Other close contacts are C2$\cdots$O3$(x - 1, y, z)$ of 3.3374 (15) Å and C2$\cdots$F1$(1 - x, 1 - y, 1 - z)$ of 3.2299 (15) Å.

The Mn—N and C—C bonds of the acetonitrile fail the rigid-bond test (Hirshfeld, 1976), with Δm.s.d.a./σ of values 8.11 and 5.24, respectively (Δm.s.d.a./σ is the difference of mean square displacement amplitudes and its standard uncertainty). The reason is obviously the nonspherical electron distribution of the triple bond, which cannot be adequately modelled with spherical scattering factors. A similar situation is well known from metal–carbonyl complexes (Braga & Koetzle, 1988). It should be noted that the absolute magnitudes for the Δm.s.d.a. values of the Mn—N and C—C bonds in (I) of 0.0041 (5) and 0.0042 (8) Å^2, respectively, are still small and well below 0.01 Å^2. A comparison with acetonitrile structures from the literature shows that the Δm.s.d.a. values of (I) are within the expected range (Table 2).

Besides the coordination chains in the a direction, the crystal structure of (I) contains layers of F atoms in the ab plane (Fig. 3). The shortest F$\cdots$F distance is F1$\cdots$F1^{iii} of 2.7796 (15) Å [symmetry code: (iii) $1 - x, 1 - y, 2 - z$], which is shorter than the sum of the van der Waals radii (2.94 Å). According to Ramasubbu *et al.* (1986) and Reichenbächer *et al.* (2005), F$\cdots$F interactions with two equal C—F$\cdots$F angles are caused by close packing (Type I), and stabilizing F$\cdots$F interactions are characterized by C—F$\cdots$F angles of 180° on one side and 90° on the other (Type II). The above-mentioned

short F$\cdots$F interaction in (I) is located on an inversion centre and consequently has two equal angles [137.69 (9)°]. The interaction is thus not stabilizing. Nevertheless, it is interesting to note that the crystals have the shape of plates with (001) as the smallest dimension, which is parallel to the fluorine layers.

Integration of the raw diffractometer images was performed using the program *EVAL15* (Schreurs *et al.*, 2010), using an accurate description of the diffraction experiment for the prediction of the reflection profiles. A relatively large isotropic mosaicity of 1.3° was used as part of this description, indicating severe defects in the crystal. Nevertheless, some equivalents of weak reflections had significant intensities, which we could interpret as Renninger effects (Renninger, 1937) (Table 3). It has been known for a long time that Renninger effects can be present in imperfect crystals (Zachariasen, 1965) and examples involving organic salts can also be found in the literature (Speakman, 1965; Grochowski *et al.* 2000). In the examples in Table 3, the intensity of one of the measurements of the $41\bar{1}$ reflection (reflA) is caused by the strong $20\bar{1}$ reflection (reflB), with $F_{calc}^2 = 3565.42$, and for the (reflB − reflA) reflection $\bar{2}10$, $F_{calc}^2 = 1400.59$. In the case of the 512 reflection, the interfering reflection is again $20\bar{1}$. Here, for the (reflB − reflA) reflection $\bar{3}13$, $F_{calc}^2 = 2387.81$.

Based on these observations, we calculated Renninger scores for all reflections. In the first instance, it is checked if the geometric condition of two reflections being simultaneously in the reflecting position is satisfied, or, in other words, whether the corresponding reciprocal lattice points are both on the Ewald sphere. This condition is fulfilled if the lengths of both reflected beam vectors are equal to the radius of the Ewald sphere within a chosen tolerance of 0.12%. A second condition is the intensity condition, meaning that (reflB) and (reflB − reflA) must both be strong. We consider a reflection as strong if the intensity is larger than $0.02F(000)_{calc}^2$. If both conditions are fulfilled, the Renninger score is calculated as

intensity(reflB) × intensity(reflB − reflA)/$[F(000)^2_{calc} × sinth]$, where sinth = $\sin(\theta)/\lambda$. We did not try to correct the affected intensities for multiple diffraction (Hauback *et al.*, 1990), but omitted all reflections with a Renninger score larger than 500 from the final data set. This omission corresponds to 3.8% of all reflections. Due to the redundant measurement this still resulted in a complete data set of unique reflections.

Experimental

Compound (I) was synthesized according to the literature procedure of Bryan & Dabrowiak (1975). Single crystals suitable for X-ray diffraction were obtained by vapour diffusion of diethyl ether into an acetonitrile solution of (I). IR (ν, cm^{-1}): 3458.5, 2950.7, 2309.5 (CH_3CN), 2280.1 (CH_3CN), 1666.5, 1632.7, 1365.7, 1302.7 (SO_3, *as*), 1228.8 (SO_3, *as*), 1210.5 (CF_3, *s*), 1184.2 (CF_3, *as*), 1031.4 (SO_3, *s*), 938.6, 799.4, 769.1.

Crystal data

$[Mn(CF_3O_3S)_2(C_2H_3N)_2]$	$\gamma = 76.025 (1)°$
$M_r = 435.19$	$V = 372.35 (1) Å^3$
Triclinic, $P\bar{1}$	$Z = 1$
$a = 5.13763 (8) Å$	Mo $K\alpha$ radiation
$b = 8.11880 (12) Å$	$\mu = 1.26 mm^{-1}$
$c = 9.75293 (10) Å$	$T = 110 K$
$\alpha = 73.126 (1)°$	$0.36 × 0.33 × 0.09 mm$
$\beta = 76.885 (1)°$	

Data collection

Nonius KappaCCD area-detector diffractometer	12368 measured reflections
Absorption correction: multi-scan (*SADABS*; Sheldrick, 2008*a*)	1710 independent reflections
$T_{min} = 0.626$, $T_{max} = 0.746$	1661 reflections with $I > 2\sigma(I)$
	$R_{int} = 0.017$

Refinement

$R[F^2 > 2\sigma(F^2)] = 0.018$	118 parameters
$wR(F^2) = 0.048$	All H-atom parameters refined
$S = 1.06$	$\Delta\rho_{max} = 0.46 e Å^{-3}$
1710 reflections	$\Delta\rho_{min} = -0.34 e Å^{-3}$

Table 1
Selected geometric parameters (Å, °).

Mn1—O1	2.1688 (8)	S1—O3	1.4283 (9)
Mn1—O2^i	2.1734 (8)	S1—O1	1.4534 (8)
Mn1—N1	2.2106 (10)	S1—O2	1.4564 (8)
O1—Mn1—O2^i	89.59 (3)	C2—N1—Mn1	153.27 (9)
O1—Mn1—N1	91.38 (4)		
O3—S1—C1—F2	58.46 (12)	O2—S1—C1—F1	56.36 (12)
O2—S1—C1—F2	−63.53 (11)	O3—S1—C1—F3	−60.98 (11)
O1—S1—C1—F1	−61.11 (12)	O1—S1—C1—F3	59.57 (11)

Symmetry code: (i) $x − 1, y, z$.

H atoms were located in difference Fourier maps and refined freely with isotropic displacement parameters [C—H = 0.90 (3)–0.94 (3) Å].

Data collection: *COLLECT* (Nonius, 1999); cell refinement: *PEAKREF* (Schreurs, 2005); data reduction: *EVAL15* (Schreurs *et al.*, 2010) and *SADABS* (Sheldrick, 2008*a*); program(s) used to solve

Table 2
Hirshfeld rigid-bond tests (Hirshfeld, 1976) of metal-coordinated acetonitrile – comparison of (I) with structures extracted from *Acta Crystallographica Section C*.

The structures are identified by their refcode in the Cambridge Structural Database (Allen, 2002). Structures with Δm.s.d.a./$\sigma > 5$ are marked with a hash sign (#). Only one acetonitrile is considered if the structure contains several coordinated acetonitriles (refcodes LIYXUM, NAQMUN01, PAJKER, QILXOY and YOJJIQ).

CSD refcode	T (K)	Max sin (θ/λ) (Å^{-1})	M	Δm.s.d.a. ($M \cdots N$) (Å^2)	Δm.s.d.a. (N—C) (Å^2)	Δm.s.d.a. (C—C) (Å^2)
(I)	110 (2)	0.65	Mn	0.0041 (5)#	0.0021 (7)	0.0042 (8)#
AHIFUS	150 (2)	0.91	Rh	0.0024 (4)#	0.0007 (6)	0.0021 (9)
DIKQIY	296	0.66	Ru	0.0092 (27)	0.0021 (43)	0.0064 (57)
GUGTEH	158 (2)	0.63	Co	0.0059 (27)	0.0017 (40)	0.0038 (42)
GUGWIO	180 (2)	0.67	Cu	0.0122 (14)#	0.0060 (23)	0.0056 (33)
IHEJUA	193 (2)	0.66	Cu	0.0009 (18)	0.0080 (26)	0.0109 (33)
JESQAA	193 (2)	0.65	Zn	0.0068 (8)#	0.0019 (11)	0.0032 (15)
LIYXUM	193 (2)	0.60	Ru	0.0008 (30)	0.0171 (50)	0.0087 (67)
MATMOJ	100.0 (10)	0.62	Ru	0.0083 (13)#	0.0041 (20)	0.0029 (27)
MEVRAG	293 (2)	0.64	Cu	0.0043 (15)	0.0047 (22)	0.0041 (23)
NAQMUN01	156 (2)	0.76	Cu	0.0025 (17)	0.0025 (24)	0.0059 (26)
OLIYEN	120 (2)	0.65	Cu	0.0033 (20)	0.0004 (28)	0.0000 (42)
PAJKER	110 (2)	0.63	Ag	0.0035 (18)	0.0073 (26)	0.0071 (28)
QANGAO	571 (2)	0.60	Cu	0.0033 (30)	0.0054 (42)	0.0074 (55)
QILXOY	150 (2)	0.63	Cu	0.0060 (8)#	0.0041 (13)	0.0051 (19)
SETPOX	296	0.62	Ru	0.0093 (27)	0.0034 (45)	0.0006 (73)
WIZDOZ	298 (2)	0.60	Cu	0.0006 (57)	0.0037 (80)	0.0053 (83)
XORVIJ	150 (2)	0.65	Cu	0.0091 (13)#	0.0012 (19)	0.0039 (22)
YOJJIQ	298 (2)	0.62	Ru	0.0065 (13)	0.0023 (21)	0.0046 (31)

Table 3
Examples of weak reflections influenced by Renninger effects.

F^2_{meas} and $\sigma(F^2_{meas})$ are taken from the raw data after integration using *EVAL15* (Schreurs *et al.*, 2010) and before the application of *SADABS* (Sheldrick, 2008*a*). For a definition of the Renninger score, see the *Comment*.

hkl	F^2_{calc}	F^2_{meas}	$\sigma(F^2_{meas})$	I/σ	Renninger score
$41\bar{1}$	0.33	17.36	0.57	30.46	1253.46
$41\bar{1}$	0.33	1.30	0.25	5.20	0.00
$41\bar{1}$	0.33	0.51	0.20	2.55	0.00
$41\bar{1}$	0.33	1.15	0.25	4.60	0.00
$41\bar{1}$	0.33	0.50	0.19	2.63	0.00
$\bar{5}1\bar{2}$	0.36	0.80	0.32	2.50	0.00
$\bar{5}12$	0.36	0.71	0.24	2.96	0.00
512	0.36	8.90	0.52	17.12	1368.45
512	0.36	0.22	0.29	0.76	0.00
512	0.36	0.62	0.27	2.30	0.00
512	0.36	0.19	0.28	0.68	0.00

structure: *SHELXS97* (Sheldrick, 2008*b*); program(s) used to refine structure: *SHELXL97* (Sheldrick, 2008*b*); molecular graphics: *PLATON* (Spek, 2009); software used to prepare material for publication: *SHELXL97*.

Supplementary data for this paper are available from the IUCr electronic archives (Reference: FG3146). Services for accessing these data are described at the back of the journal.

metal-organic compounds

References

Allen, F. H. (2002). *Acta Cryst.* B**58**, 380–388.
Berben, L. A. & Peters, J. C. (2008). *Inorg. Chem.* **47**, 11669–11679.
Bondi, A. (1964). *J. Phys. Chem.* **68**, 441–451.
Braga, D. & Koetzle, T. F. (1988). *Acta Cryst.* B**44**, 151–156.
Bryan, P. S. & Dabrowiak, J. C. (1975). *Inorg. Chem.* **14**, 296–299.
Dunitz, J. D. (1995). *X-ray Analysis and the Structure of Organic Molecules*, 2nd Corrected Reprint, pp. 106–111. Basel: Verlag Helvetica Chimica Acta.
Grochowski, J., Hupe, A., Krane, H.-G., Rossmanith, E., Schmidt, H. & Serda, P. (2000). HASYLAB Jahresber. http://www1.uni-hamburg.de/mpi/rossmanith/Reprints/hasy_00a.pdf
Hauback, B. C., Mo, F. & Thorkildsen, G. (1990). *Aust. J. Phys.* **43**, 77–91.
Hirshfeld, F. L. (1976). *Acta Cryst.* A**32**, 239–244.
Kitajgorodskij, A. I. (1973). In *Molecular Crystals and Molecules*. New York: Academic Press.
Murthy, N. N., Mahroof-Tahir, M. & Karlin, K. D. (2001). *Inorg. Chem.* **40**, 628–635.
Nonius (1999). *COLLECT*. Nonius BV, Delft, The Netherlands.
Ramasubbu, N., Parthasarathy, R. & Murray-Rust, P. (1986). *J. Am. Chem. Soc.* **108**, 4308–4314.
Reichenbächer, K., Süss, H. I. & Hulliger, J. (2005). *Chem. Soc. Rev.* **34**, 22–30.
Renninger, M. (1937). *Z. Phys.* **106**, 141–176.
Robinson, K., Gibbs, G. V. & Ribbe, P. H. (1971). *Science*, **172**, 567–570.
Schreurs, A. M. M. (2005). *PEAKREF*. Utrecht University, The Netherlands.
Schreurs, A. M. M., Xian, X. & Kroon-Batenburg, L. M. J. (2010). *J. Appl. Cryst.* **43**. In the press. doi:10.1107/S0021889809043234.
Sheldrick, G. M. (2008a). *SADABS*. University of Göttingen, Germany.
Sheldrick, G. M. (2008b). *Acta Cryst.* A**64**, 112–122.
Speakman, J. C. (1965). *Acta Cryst.* **18**, 570–571.
Spek, A. L. (2009). *Acta Cryst.* D**65**, 148–155.
Weller, F., Mai, H.-J. & Dehnicke, K. (1996). *Z. Naturforsch. Teil B*, **51**, 298–300.
Zachariasen, W. H. (1965). *Acta Cryst.* **18**, 705–710.